Available online at www.sciencedirect.com

ScienceDirect

Energy Procedia 142 (2017) 971–976

Energy Procedia

www.elsevier.com/locate/procedia

9th International Conference on Applied Energy, ICAE2017, 21-24 August 2017, Cardiff, UK

Reducing model complexity of DFIG-based wind turbines to improve the efficiency of power system stability analysis

S. Q. Bu[a]*, X. Zhang[b], S. W. Xia[a,c], Y. Xu[d], B. Zhou[e] and X. Lu[a]

[a]*Hong Kong Polytechnic University, Hung Hom, Kowloon, Hong Kong*
[b]*National Grid, St Catherines Lodge, Wokingham RG41 5BN, United Kingdom*
[c]*North China Electric Power University, Changping, Beijing 102206, China*
[d]*Nanyang Technological University, 50 Nanyang Avenue, Singapore 639798*
[e]*Hunan University, Yuelu, Changsha 410082, China*

Abstract

The growing number of doubly-fed induction generator (DFIG) based wind farms has significantly increased the model complexity and simulation burden for power system stability analysis. In this paper, a novel method to assess the modeling adequacy of DFIGs for small-signal stability analysis is introduced. By evaluating the damping torque contribution to stability margin from different DFIG dynamic model components, the proposed method provides a quantitative index to show the participation level of each DFIG model component in affecting power system damping performance. In addition, five DFIG model reduction schemes are established, and a novel strategy to reduce individual DFIG model complexity based on the participation level is proposed. The effectiveness of the proposed strategy has been demonstrated in the New England test system. It can be concluded that the proposed DFIG model reduction for dynamic studies is undoubtedly beneficial to system planner and operator, in the way of improving computational efficiency when analyzing large-scale power systems with the increasing penetration of wind energy.

Keywords: Computational efficiency; Damping torque contribution; Dynamic model component; Reduced model; Wind power generation.

* Corresponding author. Tel.: +852-2766-6163; fax: +852-2330-1544.
E-mail address: siqi.bu@gmail.com

1876-6102 © 2017 The Authors. Published by Elsevier Ltd.
Peer-review under responsibility of the scientific committee of the 9th International Conference on Applied Energy .
10.1016/j.egypro.2017.12.155

1. Introduction

Doubly-fed induction generator (DFIG) based wind turbine is equipped with power electronics converters, which enables its characteristic of faster response and effective control. However, the converter controllers have raised the modeling complexity of wind generation. As a result, the size of power system dynamic model could be considerably increased with the penetration of DFIGs. Since the model size can significantly affect the efficiency of dynamic stability studies, it is beneficial to reduce DFIG model complexity yet retain sufficient adequacy.

Initial study to reduce DFIG models is implemented by empirically attempting and validating different models [1-3]. Later some theoretical model order reduction techniques have been developed, e.g., selective modal analysis in [4], balanced truncation in [5] and singular perturbation analysis in [6]. However, most of model reduction techniques only focus on the dynamics of DFIG itself, with little consideration in whole system impact. In reality, Electricity System Operator needs to deal with stability issues by studying all the DFIGs' performance subject to various system operating conditions, which requires an effective model reduction strategy to improve the calculation efficiency, especially for real-time online stability analysis.

In this paper, a model reduction strategy for DFIGs is proposed based on a novel modeling adequacy assessment. Modeling adequacy assessment is used to determine participation level of damping contribution for each DFIG and its internal dynamic model component. Based on participation level, a step-by-step DFIG model reduction strategy is implemented by five model reduction schemes. Improved calculation efficiency is observed in New England test system for small-signal stability analysis.

2. Modeling adequacy assessment of DFIGs

A standard linearized model of multi-machine power system with the algebraic model of DFIGs can be written as (A detailed procedure to drive this model can be found in [8])

$$\begin{bmatrix}\Delta\dot{\boldsymbol{\delta}}\\ \Delta\dot{\boldsymbol{\omega}}\\ \Delta\dot{\boldsymbol{z}}\end{bmatrix}=\begin{bmatrix}\mathbf{0} & \omega_0\boldsymbol{I} & \mathbf{0}\\ \boldsymbol{A}_{21} & \boldsymbol{A}_{22} & \boldsymbol{A}_{23}\\ \boldsymbol{A}_{31} & \boldsymbol{A}_{32} & \boldsymbol{A}_{33}\end{bmatrix}\begin{bmatrix}\Delta\boldsymbol{\delta}\\ \Delta\boldsymbol{\omega}\\ \Delta\boldsymbol{z}\end{bmatrix}+\left[\begin{array}{c|c}\mathbf{0} & \\ \boldsymbol{B}_2 & \mathbf{0}\\ \boldsymbol{B}_3 & \end{array}\right]\left[\begin{array}{c}\Delta\boldsymbol{s}\\ \Delta\boldsymbol{E}_d\\ \Delta\boldsymbol{E}_q\\ \hline \Delta\boldsymbol{X}_c\end{array}\right] \tag{1}$$

where $\Delta\boldsymbol{\delta}$ and $\Delta\boldsymbol{\omega}$ is the vector of variation of power angle and angular speed of synchronous generators (SGs) respectively, and Δz is the vector of other state variables of SGs. $\Delta\boldsymbol{s}$, $\Delta\boldsymbol{E_d}$ and $\Delta\boldsymbol{E_q}$ is the vector of variation of slip and electromotive force of DFIGs. $\Delta\boldsymbol{X_c}$ is the vector of state variables of converter integral controllers as well as the DC link of DFIGs. It can be noted from (1) that $\Delta\boldsymbol{X_c}$ does not have a direct contribution to the system damping.

The internal dynamics of DFIGs includes dynamics of induction generator, rotor-side converter (RSC) controller, grid-side converter (GSC) controller and DC link. The generic DFIG differential equations can be written as

$$\begin{bmatrix}\Delta\dot{\boldsymbol{s}}\\ \Delta\dot{\boldsymbol{E}}_d\\ \Delta\dot{\boldsymbol{E}}_q\\ \Delta\dot{\boldsymbol{X}}_c\end{bmatrix}\begin{bmatrix}\boldsymbol{A}_{11w} & \boldsymbol{A}_{12w} & \mathbf{0} & \mathbf{0}\\ \mathbf{0} & \boldsymbol{A}_{22w} & \mathbf{0} & \boldsymbol{A}_{24w}\\ \mathbf{0} & \mathbf{0} & \boldsymbol{A}_{33w} & \boldsymbol{A}_{34w}\\ \boldsymbol{A}_{41w} & \boldsymbol{A}_{42w} & \boldsymbol{A}_{43w} & \boldsymbol{A}_{44w}\end{bmatrix}\begin{bmatrix}\Delta\boldsymbol{s}\\ \Delta\boldsymbol{E}_d\\ \Delta\boldsymbol{E}_q\\ \Delta\boldsymbol{X}_c\end{bmatrix}+\begin{bmatrix}\boldsymbol{B}_{1w}\\ \boldsymbol{B}_{2w}\\ \boldsymbol{B}_{3w}\\ \boldsymbol{B}_{4w}\end{bmatrix}\Delta\boldsymbol{V}_w \tag{2}$$

According to (1), the forward path function from $\left[\Delta\boldsymbol{s},\Delta\boldsymbol{E}_d,\Delta\boldsymbol{E}_q\right]^{\boldsymbol{T}}$ to electric torque of SGs is

$$\boldsymbol{F}_w(p)=\boldsymbol{A}_{23}(p\boldsymbol{I}-\boldsymbol{A}_{33})^{-1}\boldsymbol{B}_3+\boldsymbol{B}_2 \tag{3}$$

where $\boldsymbol{F}_w(p)$ is a $m\times 3l$ matrix, assuming there are totally m SGs and l DFIGs in the system.

Based on (2), the contributions from $\Delta\boldsymbol{V}_w$ to $\left[\Delta\boldsymbol{s},\Delta\boldsymbol{E}_d,\Delta\boldsymbol{E}_q\right]^{\boldsymbol{T}}$ can be computed and the dynamics of DFIGs can be split and described by three separate transfer functions

$$\begin{cases}\boldsymbol{G}_{\boldsymbol{E}_d}(p)=[\boldsymbol{I}-(p\boldsymbol{I}-\boldsymbol{A}_{22w})^{-1}\boldsymbol{A}_{24w}(p\boldsymbol{I}-\boldsymbol{A}_{44w})^{-1}\boldsymbol{A}_{42w}]^{-1}\times(p\boldsymbol{I}-\boldsymbol{A}_{22w})^{-1}[\boldsymbol{A}_{24w}(p\boldsymbol{I}-\boldsymbol{A}_{44w})^{-1}\boldsymbol{B}_{4w}+\boldsymbol{B}_{2w}]\\ \boldsymbol{G}_{\boldsymbol{E}_q}(p)=[\boldsymbol{I}-(p\boldsymbol{I}-\boldsymbol{A}_{33w})^{-1}\boldsymbol{A}_{34w}(p\boldsymbol{I}-\boldsymbol{A}_{44w})^{-1}\boldsymbol{A}_{43w}]^{-1}\times(p\boldsymbol{I}-\boldsymbol{A}_{33w})^{-1}[\boldsymbol{A}_{34w}(p\boldsymbol{I}-\boldsymbol{A}_{44w})^{-1}\boldsymbol{B}_{4w}+\boldsymbol{B}_{3w}]\\ \boldsymbol{G}_s(p)=(p\boldsymbol{I}-\boldsymbol{A}_{11w})^{-1}\left[\boldsymbol{B}_{1w}+\boldsymbol{A}_{12w}\boldsymbol{G}_{\boldsymbol{E}_d}(p)\right]\end{cases} \tag{4}$$

where $\boldsymbol{G}_{\boldsymbol{E}_d}(p)_{l\times 2l}=\Delta\boldsymbol{E}_d/\Delta\boldsymbol{V}_w$, $\boldsymbol{G}_{\boldsymbol{E}_q}(p)_{l\times 2l}=\Delta\boldsymbol{E}_q/\Delta\boldsymbol{V}_w$, and $\boldsymbol{G}_s(p)_{l\times 2l}=\Delta\boldsymbol{s}/\Delta\boldsymbol{V}_w$. As proved by (1) previously that the dynamics of integral controllers and DC link of DFIG converter do not have a direct impact on system damping, it actually contributes the system damping via the channel of $\left[\Delta\boldsymbol{s}, \Delta\boldsymbol{E_d}, \Delta\boldsymbol{E_q}\right]^{\boldsymbol{T}}$. Therefore, both damping contributions of $\Delta\boldsymbol{E_d}$ and $\Delta\boldsymbol{E_q}$ consist of two parts: the contributions from their own dynamics ($\Delta\boldsymbol{E_d}$ or $\Delta\boldsymbol{E_q}$) and dynamics of ΔX_c. It is possible to differentiate these two parts in $\boldsymbol{G_{E_d}}(p)$ and $\boldsymbol{G_{E_q}}(p)$ as well as $\boldsymbol{G_s}(p)$

$$\begin{cases}\boldsymbol{G_{E_d\_E_d}}(p) = (p\boldsymbol{I} - \boldsymbol{A_{22w}})^{-1}\boldsymbol{B_{2w}}, \boldsymbol{G_{E_d\_X_c}}(p) = \boldsymbol{G_{E_d}}(p) - \boldsymbol{G_{E_d\_E_d}}(p) \\ \boldsymbol{G_{E_q\_E_q}}(p) = (p\boldsymbol{I} - \boldsymbol{A_{33w}})^{-1}\boldsymbol{B_{3w}}, \boldsymbol{G_{E_q\_X_c}}(p) = \boldsymbol{G_{E_q}}(p) - \boldsymbol{G_{E_q\_E_q}}(p) \\ \boldsymbol{G_{s\_sE_d}}(p) = (p\boldsymbol{I} - \boldsymbol{A_{11w}})^{-1}\left[\boldsymbol{B_{1w}} + \boldsymbol{A_{12w}}\boldsymbol{G_{E_d\_E_d}}(p)\right], \boldsymbol{G_{s\_X_c}}(p) = (p\boldsymbol{I} - \boldsymbol{A_{11w}})^{-1}\,\boldsymbol{A_{12w}}\boldsymbol{G_{E_d\_X_c}}(p)\end{cases} \tag{5}$$

Assuming the i^{th} eigenvalue λ_i is the critical oscillation mode in the system, $\Delta\boldsymbol{V_w}$ should be equal to $\boldsymbol{\gamma_{ik}}\Delta\omega_k$ [7], and thus combining (3) and (4), the electric torque provided by DFIGs to the k^{th} SG can be written as

$$\Delta T_{wk} = \boldsymbol{F_{wk}}(\lambda_i)[\boldsymbol{G_s}(\lambda_i), \boldsymbol{G_{E_d}}(\lambda_i), \boldsymbol{G_{E_q}}(p\lambda_i)]^{\boldsymbol{T}}\boldsymbol{\gamma_{ik}}\Delta\omega_k \tag{6}$$

where $\boldsymbol{F_{wk}}(p)$ is the k^{th} row of $\boldsymbol{F_w}(p)$. Eq. (6) can be further factorized to torque contribution of each dynamic model component of each DFIG by using (5). The electric torque from dynamics of the j^{th} DFIG to the k^{th} SG is

$$\begin{cases}\Delta T_{wkj\_s} = F_{wkj\_s}(\lambda_i)\boldsymbol{G_{s\_sE_dj}}(\lambda_i)\boldsymbol{\gamma_{ijk}}\Delta\omega_k \\ \Delta T_{wkj\_E_d} = F_{wkj\_E_d}(\lambda_i)\boldsymbol{G_{E_d\_E_dj}}(\lambda_i)\boldsymbol{\gamma_{ijk}}\Delta\omega_k \\ \Delta T_{wkj\_E_q} = F_{wkj\_E_q}(\lambda_i)\boldsymbol{G_{E_q\_E_qj}}(\lambda_i)\boldsymbol{\gamma_{ijk}}\Delta\omega_k \\ \Delta T_{wkj\_X_c} = [F_{wkj\_E_d}(\lambda_i)\boldsymbol{G_{E_d\_X_cj}}(\lambda_i) + F_{wkj\_E_q}(\lambda_i)\boldsymbol{G_{E_q\_X_cj}}(\lambda_i) + F_{wkj\_s}(\lambda_i)\boldsymbol{G_{s\_X_cj}}(\lambda_i)]\boldsymbol{\gamma_{ijk}}\Delta\omega_k\end{cases} \tag{7}$$

where the subscript j, s, E_d, E_q and X_c denote the relevant part of matrices associated with different dynamics of the j^{th} DFIG, $\Delta T_{wkj} = \Delta T_{wkj\_s} + \Delta T_{wkj\_E_d} + \Delta T_{wkj\_E_q} + \Delta T_{wkj\_X_c}$ and $\Delta T_{wk} = \sum_{j=1}^{l} \Delta T_{wkj}$. Hence, the impact of DFIG dynamics on λ_i can be assessed by introducing S_{ik}, the sensitivity of λ_i w.r.t. the electric torque coefficient [7].

$$\Delta\lambda_i = \sum_{k=1}^{m} S_{ik}TC_{wk} = \sum_{k=1}^{m} S_{ik}\sum_{j=1}^{l} TC_{wkj} = \sum_{k=1}^{m} S_{ik}\sum_{j=1}^{l}\left(TC_{wkj\_s} + TC_{wkj\_E_d} + TC_{wkj\_E_q} + TC_{wkj\_X_c}\right) \tag{8}$$

where TC_{wk} and TC_{wkj} is the electric torque coefficient of ΔT_{wk} and ΔT_{wkj}, and $TC_{wkj\_s}, TC_{wkj\_E_d}, TC_{wkj\_E_q}$ and $TC_{wkj\_X_c}$ is the coefficient of each dynamic model component in (7).

In (8), the participation level in contributing damping is ranked for each DFIG's dynamic model components by their contributions to the critical eigenvalue. The participation level is able to indicate which part of DFIG dynamics can be ignored in the small-signal stability analysis due to less involvement in dynamic interactions. Based on modelling adequacy assessment results, a model reduction strategy of DFIGs is proposed in Section 3.

3. Model reduction strategy for DFIGs

Based on different participation level of dynamic model components in DFIGs, five gradually reduced models are established step by step in the following.

3.1. *Reduction of dynamics of $\Delta\boldsymbol{X_c}$ (constant $\boldsymbol{X_c}$ model)*

As discussed previously in (1), $\Delta\boldsymbol{X_c}$ (the dynamics of integral controller and DC link only) impacts the system indirectly by contributing damping to $\left[\Delta\boldsymbol{s}, \Delta\boldsymbol{E_d}, \Delta\boldsymbol{E_q}\right]^{\boldsymbol{T}}$ **.**and hence if $\Delta\boldsymbol{X_c}$ has a high participation in affecting small-signal stability margin which cannot be ignored, the dynamic model of $\left[\Delta\boldsymbol{s}, \Delta\boldsymbol{E_d}, \Delta\boldsymbol{E_q}\right]^{\boldsymbol{T}}$ cannot be reduced. Therefore, the reduction of dynamics of $\Delta\boldsymbol{X_c}$ is considered as the first step of the DFIG model reduction. For demonstration purpose, in the rest of this subsection assume there is only one DFIG in the system. The dynamics of $\Delta\boldsymbol{X_c}$ can be neglected when the participation level of $\Delta\boldsymbol{X_c}$ is below certain threshold. The resultant linearized dynamic model in (2) is reduced to

$$\begin{bmatrix}\Delta\dot{s} \\ \Delta\dot{E}_d \\ \Delta\dot{E}_q\end{bmatrix} = \begin{bmatrix}A_{11w} & A_{12w} & 0 \\ 0 & A_{22w} & 0 \\ 0 & 0 & A_{33w}\end{bmatrix}\begin{bmatrix}\Delta s \\ \Delta E_d \\ \Delta E_q\end{bmatrix} + \begin{bmatrix}\boldsymbol{B_{1w}} \\ \boldsymbol{B_{2w}} \\ \boldsymbol{B_{3w}}\end{bmatrix}\Delta\boldsymbol{V_w} \tag{9}$$

3.2. *Reduction of dynamics of* $\Delta \boldsymbol{X_c}$ *and* Δs *(constant* $\boldsymbol{X_c}$ *and s model)*

The third-order model shown in (9) is the most commonly used simplified model of DFIGs in the existing research. By applying the modeling adequacy assessment, it has been discovered in this paper that the third-order model can be further reduced. When the participation level of both $\Delta \boldsymbol{X_c}$ and Δs is below certain threshold, the dynamics of $\Delta \boldsymbol{X_c}$ and Δs can be neglected at the same time and the linearized dynamic model becomes (10). The electric torque is considered to be equal to the mechanical torque in this model so that the rotor speed could stay constant.

$$\begin{bmatrix} \Delta \dot{E}_d \\ \Delta \dot{E}_q \end{bmatrix} = \begin{bmatrix} A_{22w} & 0 \\ 0 & A_{33w} \end{bmatrix} \begin{bmatrix} \Delta E_d \\ \Delta E_q \end{bmatrix} + \begin{bmatrix} \boldsymbol{B_{2w}} \\ \boldsymbol{B_{3w}} \end{bmatrix} \Delta \boldsymbol{V_w} \tag{10}$$

3.3. *Reduction of dynamics of* $\Delta \boldsymbol{X_c}, \Delta E_d$ *and* ΔE_q *(constant* $\boldsymbol{X_c}$ *and* $\Delta \dot{E} = 0$ *model)*

On the basis of model reduction presented in 3.1, the dynamics of rotor flux represented by ΔE_d *and* ΔE_q can be further neglected by setting $\Delta \dot{E_d} = 0$ and $\Delta \dot{E_q} = 0$ in small-signal stability analysis [9]. Due to the existence of offset voltage items in RSC controller, the physical meaning of $\Delta \dot{E_d} = 0$ and $\Delta \dot{E_q} = 0$ is that the dynamics of inner current loop of RSC controller is ignored and the rotor current can track its reference instantaneously. This reduction is usually considered to be reasonable in small-signal stability analysis as the inner current loop responses much faster than the electromechanical transient [9]. As a result, $\Delta \mathrm{E_d}$ and $\Delta \mathrm{E_q}$ become algebraic variables like terminal voltage and the dynamic model associated with $\Delta \mathrm{E_d}$ and $\Delta \mathrm{E_q}$ in (9) becomes algebraic model. It is straight forward to assess the impact of the reduction of rotor flux dynamics on the critical eigenvalue by simply setting $p = 0$ for $(p\boldsymbol{I} - \boldsymbol{A_{22w}})^{-1}$ and $(p\boldsymbol{I} - \boldsymbol{A_{33w}})^{-1}$ in (4) and (5). It can be concluded that further reductions on the dynamics of ΔE_d and ΔE_q could be carried out if the change in their participation levels (before and after $p = 0$) are less than the preset threshold.

3.4. *Reduction of dynamics of* $\Delta \boldsymbol{X_c}, \Delta s, \Delta E_d$ *and* ΔE_q *(constant* $\boldsymbol{X_c}$*, s and* $\Delta \dot{E} = 0$ *model)*

Similarly, if the requirement of dynamics reduction in 3.2 and 3.3 are met simultaneously, the model reductions can be combined and the dynamic model of the DFIG becomes a pure algebraic model without differential equations. That is to say, the introduction of constant $\boldsymbol{X_c}$, s and $\Delta \dot{E} = 0$ model of DFIGs to the system would not increase the computational time. Similar to 3.3, this model can be derived from the constant $\boldsymbol{X_c}$ and s model by setting $p = 0$.

3.5. *Reduction of dynamics of* $\Delta \boldsymbol{X_c}, \Delta s, \Delta E_d$ *and* ΔE_q *(constant* $\boldsymbol{X_c}$*, s and E model)*

If the participation level of all the state variables of the DFIG in affecting the critical eigenvalue is very low, all dynamics of the DFIG can be removed in the study. In this case, the DFIG can be modeled as a constant admittance with constant $\boldsymbol{X_c}$, s, E_d and E_q.

The model reduction schemes in 3.1-3.5 apply to the individual DFIG level. On this basis, a model reduction strategy is proposed for multiple grid-connected DFIGs on the system level, aiming to reduce the complexity of overall system dynamic model. The model reduction should start from the dynamic model of DFIGs with comparatively low-level participation. For instance, some small-scale DFIG-based wind farms are located far away from main-interconnected system, the dynamics of which might have a limited impact on the critical eigenvalue and thus could be generally ignored. A concept of model reduction margin (MRM) determined by the preset variation of damping ratio of the critical eigenvalue is proposed to define the maximal damping variation (either +ve or -ve) allowed in the model reduction. If the critical eigenvalue $\lambda_i = \sigma + j\omega$ and the damping ratio is denoted as ζ,

$$\mathrm{MRM} = \left| \frac{\mathrm{a}\%\omega}{\sqrt{1-(\mathrm{a}\%)^2}} \right| \tag{11}$$

where a% is the preset variation of ζ (e.g., the variation range allowed for ζ is from 2.97% to 3.03% if a% is set to 0.03% and $\zeta = 3\%$). Therefore, once a% is set up and MRM is calculated according to (11). DFIGs are ranked and numbered based on their respective participation level from low to high after the modeling adequacy assessment. The model reduction is implemented from the DFIGs with low-level participation to the ones with high-level participation. For each DFIG, different model reduction schemes are tried on generator level and the reduced model with less orders has the higher priority as long as the total damping variation is still within MRM. The model reduction stops when MRM is reached and the most effective model reduction strategy for the system is finalized.

4. Application

The New England test system (NETS) with 10 SGs and 39 buses is used to demonstrate the proposed model reduction strategy in Fig. 1. A detailed twelfth-order DFIG model [7] consisting of third-order induction generator, fourth-order RSC controller, fourth-order GSC controller and first-order DC link is employed as a benchmark model with corresponding parameters below. Three DFIG-based wind farms (WF1-3) are connected to bus 19, 30 and 36. The output active power and terminal voltage of the three DFIGs are also provided.

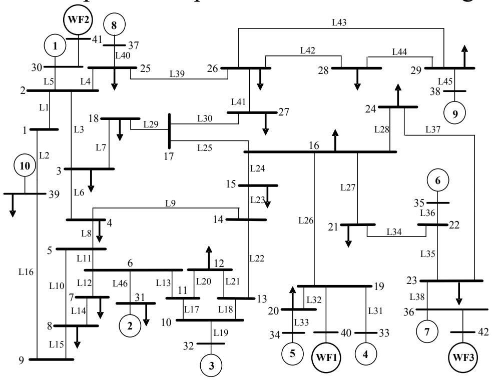

Induction generator parameters
$S_{DFIG} = 70MVA, M_w = 3.4s, D_w = 0, R_r = 0.0007, X_s = 0.0878, X_r = 0.0373, X_m = 1.3246, X_{r3} = 0.05, V_{dc0} = 1, C_{GSC} = 13.29$
RSC controller parameters
$K_{psp1} = K_{qsp1} = 0.2, K_{psp2} = K_{qsp2} = 1, K_{psI1} = K_{qsI1} = 12.56s^{-1}, K_{psI2} = K_{qsI2} = 62.5s^{-1}$
GSC controller parameters
$K_{vdcp1} = K_{qr3p1} = 0.2, K_{vdcp2} = K_{qr3p2} = 1, K_{vdcI1} = K_{qr3I1} = 12.56s^{-1}, K_{vdcI2} = K_{qr3I2} = 62.5s^{-1}$
Operational Conditions
$P_{w1} = P_{w2} = P_{w3} = 2.0\,p.u., V_{w1} = V_{w2} = V_{w3} = 1.025\,p.u.$

Fig. 1. Diagram of 10-machine 39-bus New England test system integrated with 3 WFs.

In this case, the 17th eigenvalue λ_{17} is regarded as the critical eigenvalue as an example. The critical eigenvalue reflects the inter-area oscillation mode between NETS represented by SG1-9 and external power system (New York power system) represented by the equivalent generator SG10 of the external system. When the DFIGs are connected, if only considering the impact of the constant admittance of the DFIGs, by computing the critical eigenvalue of state matrix in (1), $\lambda_{17}^{CA} = -0.1199 + \text{j}3.2452$. Then the modeling adequacy assessment is implemented and the contributions from different dynamics of DFIGs to the critical eigenvalue are computed by (8), and presented in Table 1. The real part of the eigenvalue contribution in Table I indicates the participation of each dynamic model component of the DFIGs in affecting the system damping. It can be revealed that different connecting locations lead to different participation levels of DFIG dynamics. According to (8), the eigenvalue contribution from the dynamics of all DFIGs in Table 1 is summed up, i.e., $\Delta\lambda_{17} = 0.0438 - \text{j}0.1012$. Finally, the critical eigenvalue considering the impact of the constant admittance and dynamics of the DFIGs can be estimated to be $\lambda_{17}^{CA} + \Delta\lambda_{17} = -0.0761 + \text{j}3.1440$.

Table 1. Eigenvalue contributions from different DFIG dynamics.

$\Delta\lambda_{17}$	From WF1	From WF2	From WF3
Δs	$-8.2633 \times 10^{-5} + j1.1072 \times 10^{-5}$	$-1.5575 \times 10^{-5} - j1.0050 \times 10^{-5}$	$-5.2153 \times 10^{-5} - j1.6774 \times 10^{-5}$
ΔE_d	$-8.9922 \times 10^{-5} - j4.0514 \times 10^{-4}$	$4.5767 \times 10^{-5} - j8.7290 \times 10^{-5}$	$6.2514 \times 10^{-5} - j2.7911 \times 10^{-4}$
ΔE_q	$0.0192 - j0.0733$	$0.0109 - j0.0072$	$0.0128 - j0.0180$
$\Delta \boldsymbol{X_c}$	$0.0005 - j0.0014$	$2.2901 \times 10^{-4} - j1.2328 \times 10^{-4}$	$2.8821 \times 10^{-4} - j3.3864 \times 10^{-4}$
Total	$0.0196 - j0.0751$	$0.0111 - j0.0074$	$0.0131 - j0.0187$

To validate the method above, modal analysis is carried out and the critical eigenvalue of the complete linearized model of the test system with DFIGs can be obtained, i.e., $\lambda_{17}^{MA} = -0.0760 + j3.1448$. By comparing λ_{17}^{MA} and $\lambda_{17}^{CA} + \Delta\lambda_{17}$, the accuracy and effectiveness of the proposed assessment method can be verified.

Based on modeling adequacy assessment, the dynamic model of the three DFIGs is reduced by adopting the model reduction strategy. MRM is firstly calculated to be 6.2896×10^{-4}, where the critical eigenvalue is equal to λ_{17}^{MA} and a% is set to 0.02%. Then the DFIGs are ranked as WF2, WF3 and WF1 according to the total participation of each DFIG as shown in Table 1 (real part of Total). Hence, the dynamic model reduction starts from WF2 due to the lowest participation level. By comparing with MRM, Model in 3.4 is selected for WF2 and Model in 3.2 for WF1. The detailed dynamic model of WF3 should be retained as the reduction of $\Delta \boldsymbol{X_c}$ dynamics will breach MRM. After the model reduction, the total damping variation is -5.6394×10^{-4}, and thus the estimated λ_{17} is $-0.0766 + \text{j}3.1459$.

To validate the model reduction strategy, time-domain simulation based on benchmark DFIG dynamic models is conducted and compared with reduced models in Fig. 2. The power angle difference between major generators associated with this critical oscillation mode is observed, and the results demonstrate that there is no significant result difference between detailed model and reduced model. The simulation time and dynamic model complexity before and after the model reduction is also compared in Table 2. The same computational resource (Intel Core i7-4790 CPUs 3.60 GHz, 32.0 GB RAM) is employed. Around one fourth of total simulation time is saved. It can be expected that time difference in Table 2 would be much more significant with larger number of DFIGs connected.

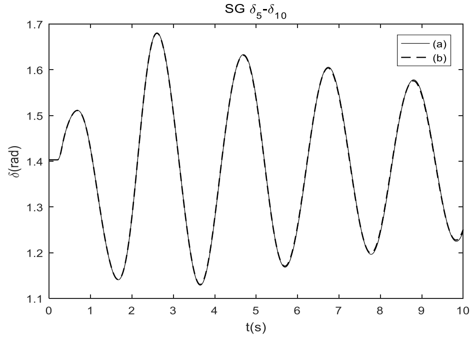

Fig. 2. SG5-SG10 power angle difference with different WF dynamic models.
(a) Three WFs with detailed model (benchmark); (b) WF1 with Model 3.2, WF2 with Model 3.4 and WF3 with detailed model.

Table 2. Simulation time before and after model reduction.

Before Reduction (76^{th}-order Model)	After Reduction (54^{th}-order Model)
93.28*s*	75.32*s*

5. Conclusions

This paper presents a novel methodology to reduce the model complexity of DFIG-based wind turbines for power system small-signal stability analysis. Model reduction strategy is achieved by the following steps: 1. Assess the modeling adequacy of DFIGs by performing the damping torque computation based on (8), to determine participation level of each component of individual DFIG in contributing system damping. 2. Sum up model component's participation level to obtain total participation level for all DFIGs (DFIGs with lower participation level contribute less to system damping, and therefore will be simplified first). 3. Five DFIG dynamic model reduction schemes are proposed to perform different levels of model reduction based on the calculated participation level. 4. Model reduction stops when MRM is reached.

Improved calculation efficiency is observed in the small-signal stability analysis of New England test system. This approves that the proposed model reduction methodology is particularly useful when analyzing dynamic stability for large-scale power systems with high penetration of wind energy. Future work will focus on the application of such DFIG model reduction techniques to the National Grid UK power network and Jiangsu power grid in China.

References

[1] J. B. Ekanayake, L. Holdsworth and N. Jenkins. Comparison of 5th order and 3rd order machine models for doubly fed induction generator (DFIG) wind turbines, Electric Power Systems Research, vol. 67, no. 3, p. 207-215, Dec. 2003.
[2] A. Feijoo J. Cidras and C. Carrillo. A third order model for the doubly-fed induction machine, Electric Power Systems Research, vol. 56, no. 2, p. 121-127, Nov. 2000.
[3] K. Elkington, V. Knazkins and M. Ghandhari. On the stability of power systems containing doubly fed induction generator-based generation, Electric Power Systems Research, vol. 78, no. 9, p. 1477-1484, Sept. 2008.
[4] H. A. Pulgar-Painemal and P. W. Sauer. Reduced-order model of type-c wind turbine generators, Electric Power Systems Research, vol. 81, no. 4, p. 840-845, Dec. 2011.
[5] S. Ghosh and N. Senroy. Balanced truncation based reduced order modeling of wind farm, International Journal of Electric Power & Energy Systems, vol. 53, p. 649-655, 2013.
[6] Y. Ni, C. Li, Z. Du and G. Zhang. Model order reduction based dynamic equivalence of a wind farm, International Journal of Electric Power & Energy Systems, vol. 83, p. 96-103, 2016.
[7] W. J. Du, J. T. Bi, J. Cao and H. F. Wang. A Method to Examine the Impact of Grid Connection of the DFIGs on Power System Electromechanical Oscillation Modes, IEEE Trans. Power Systems, vol. 31, no. 5, p. 3775-3785, Sept. 2016.
[8] X. F. Wang, Y. H. Song and M. Irving. Modern Power Systems Analysis, Berlin, Gernany: Springer, 2011.
[9] A. Ellis, Y. Kazachkov, E. Muljadi, P. Pourbeik and J. J. Sanchez-Gasca. Description and Technical Specifications for Generic WTG Models – A Status Report, IEEE PES Power Systems Conference and Exposition (PSCE) 2011, 2011, p. 1-8.